Statistical Model of Path Loss for Railway 5G Marshalling Yard Scenario

DING Jianwen[1], LIU Yao[1], LIAO Hongjian[1], SUN Bin[1], WANG Wei[2]

(1. Beijing Jiaotong University, Beijing 100044, China;
2. ZTE Corporation, Shenzhen 518057, China)

DOI: 10.12142/ZTECOM.202303015

https://link.cnki.net/urlid/34.1294.TN.20230905.2004.002, published online September 6, 2023

Manuscript received: 2022-10-25

Abstract: The railway mobile communication system is undergoing a smooth transition from the Global System for Mobile Communications-Railway (GSM-R) to the Railway 5G. In this paper, an empirical path loss model based on a large amount of measured data is established to predict the path loss in the Railway 5G marshalling yard scenario. According to the different characteristics of base station directional antennas, the antenna gain is verified. Then we propose the position of the breakpoint in the antenna propagation area, and based on the breakpoint segmentation, a large-scale statistical model for marshalling yards is established.

Keywords: 5G-R; marshalling yard; path loss prediction; statistical modeling

Citation (Format 1): DING J W, LIU Y, LIAO H J, et al. Statistical model of path loss for railway 5G marshalling yard scenario [J]. ZTE Communications, 2023, 21(3): 117 - 122. DOI: 10.12142/ZTECOM.202303015
Citation (Format 2): J. W. Ding, Y. Liu, H. J. Liao, et al., "Statistical model of path loss for railway 5G marshalling yard scenario," *ZTE Communications*, vol. 21, no. 3, pp. 117 - 122, Sept. 2023. doi: 10.12142/ZTECOM.202303015.

1 Introduction

With the deployment and advancement of the 5G "new infrastructure" strategy, a series of technological innovations for the new generation of railway mobile communication are actively being carried out in China. Taking 5G as an opportunity, 5G for Railway (5G-R) has been widely regarded as a solution to meeting the diverse requirements of railway wireless communications[1-2]. Railway 5G is composed of 5G-R and the public 5G network dedicated to the railway. Among them, 5G-R refers to a private 5G network that provides services for the railway system, which is completely independent and highly reliable. However, the current 5G-R bandwidth is limited and cannot carry a large number of high-bandwidth services in railways[3]. It is necessary to use the dedicated frequency of the public 5G network to carry out some services uncorrelated to driving safety because the 5G-R frequency has not been approved. At present, the development of the Railway 5G is in the preliminary stage, without enough technical standards for the construction of a railway wireless network. For various scenarios with higher frequencies, it is necessary to conduct a large number of field measurements and tests to collect test data. The current technical standards can be summarized and improved more accurately based on these data. Compared with the previous, the current railway system has changed a lot. Therefore, we need to determine the field strength prediction model under typical railway scenarios and provide corresponding technical standards for the construction of the Railway 5G through the evaluation of wireless network coverage. At the same time, high-speed railway is also one of the important application scenarios of the 6G mobile communication technology in the future. A 6G network can provide more comprehensive performance indicators, such as ultra-low delay jitter, ultra-high security, stereo coverage, and ultra-high positioning accuracy. With the help of 6G, more high-speed railway business and application requirements can be realized, and the development of railway digitalization can be promoted[4]. Therefore, we not only need to build a 5G-R network in an all-round way, but also make theoretical and technical preparations for 6G.

The channel parameters of 5G including path loss exponent and shadow fading were measured in the scene of campus in Ref. [5]. A new path loss prediction model for the viaduct area was deduced through statistical analysis of the measurement results in Ref. [6]. To model the path loss of viaducts and plains, Ref. [7] proposed a modified free space model with good results. The authors in Ref. [8] divided viaducts into four areas: suburban, open, mountainous and urban. They calculated respective path loss exponent and standard deviations of shadow fading. Ref. [9] measured and analyzed the path loss

This work was supported in part by the Fundamental Research Funds for the Central Universities under Grant No. 2022JBXT001, in part by NSFC under Grant No. 62171021, in part by the Project of China State Railway Group under Grant No. P2021G012, and in part by ZTE Industry-University-Institute Cooperation Funds under Grant No. I21L00220.

for the 915 MHz railway yard environment. For the scenarios of high-speed railway noise barriers and forests, the channel characteristics including delay spread and Doppler spread were analyzed based on ray tracing in Ref. [10]. On the basis of Ref. [10], the authors utilized multiple antennas for modeling and supplemented the discussion of received power in Ref. [11]. Curved and straight tunnels were measured at 900 MHz and 2 100 MHz, and the path loss modeling under train-to-train (T2T) communication was fitted[12]; Based on ray tracing simulation technology, the channel parameters such as path loss, delay spread, and Doppler spread under the 5G system in the urban rail viaduct scenario were analyzed[13].

The main contributions made in this paper are summarized as follows.

Considering the influence of the main lobe and side lobe of the directional antenna pattern of a base station, two methods of dividing the propagation area are proposed: one is based on the side lobe and main lobe coverage area division, and the other is based on the center of the main lobe of the antenna pattern. And the above two methods were compared with the Fresnel band gap division method.

Based on the field strength data measured in the actual marshalling yard scene, the above-mentioned conjecture of the division of the propagation area is verified, and a large-scale fading empirical model is established. The radio wave propagation area is divided into Area A and Area B for segmental modeling.

It is concluded that the path loss model of Area A is similar to the two-path model, and that of Area B is consistent with the traditional empirical model of large-scale fading.

Combined with the Hata model, the relationship between the correction factor and the antenna height of the base station in the marshalling station scenario is fitted. Then we propose a correction factor for Area B and establish an empirical model about this area.

2 Data Preprocessing

2.1 Antenna Gain Check

The effects of the main lobe and side lobes of the antenna pattern should be taken into account to build an accurate path loss model. By verifying the antenna gain of the original data samples, the application scope of the model can be expanded effectively. Firstly, we verify the original measurement data to obtain the received power of the reference signal at the test point. The path loss of the test point is given by

$$PL(d) = P_t - P_r(d) + G(d,\theta_1) - L_{\text{loss}}, \quad (1)$$

where P_t defines the reference signal transmitting power, $P_r(d)$ is the test point reference signal received power, L_{loss} denotes the feeder and its connection loss in the test system, and $G(d,\theta_1)$ expresses the vertical gain sum of the transmitting and receiving antennas of the base station.

The horizontal beam of the transmitting antenna we adopted is wide, and the receiving antenna is a horizontal omnidirectional antenna. The antennas are linear coverage in the scenario of a marshalling yard. It can be approximately considered that the gain of the transmitting and receiving antennas is invariable on the horizontal plane. Therefore, only the vertical antenna pattern is considered and the horizontal is irrespective in this paper.

Result $PL(d)$ obtained after antenna gain verification is the sum of path loss and shadow fading. Relative to the transmitting antenna, the receiving antenna moves slowly and the shadow fading has less effect on the overall results. Therefore, a large-scale path loss model is built based on the results obtained through antenna gain verification in the following work of this paper.

2.2 Radio Wave Propagation Area Division

The base station antennas generally used in the construction of rail transit wireless communication systems are high-gain directional antennas. Directional antennas are characterized by a small coverage angle, strong directivity, and a large signal gap between the main lobe and the side lobe. Fig. 1 is a 2D schematic diagram of a directional antenna system, where θ_1 denotes the downtilt angle of the base station antenna, taking into account both mechanical downtilt and electrical downtilt, and θ_2 denotes the 3 dB lobe width of the base station antenna in the vertical direction.

In Fig. 1, Point O represents the location of the base station tower, Point A represents the position of the vertical side lobe edge of antenna, and Point B represents the center position of the vertical main lobe of antenna. In other words, the direction of the base station antenna pointing to Point B is the main radiation direction of the antenna, which indicates the direction with the largest gain in the antenna pattern. Generally, the gain of the directional antenna pattern is large and uniform in the main lobe, while the gain in the side lobes is small and fluctuates greatly. The main lobe and side lobes will have a great impact on the received power. The antenna pattern of the transceiver antenna should be considered as a whole to ensure accurate results.

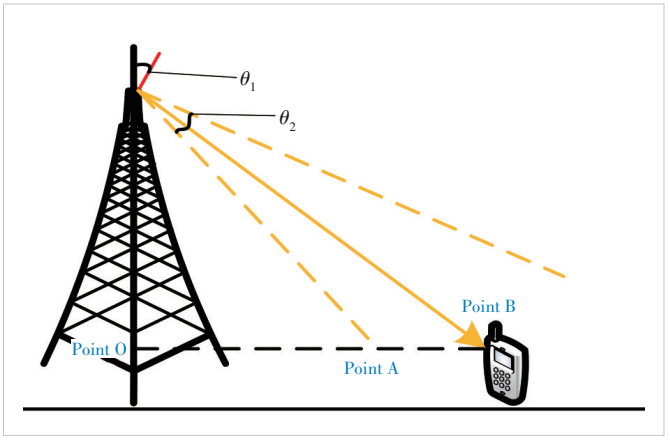

▲Figure 1. 2D schematic diagram of directional antenna system

The antenna pattern in the near-field area of the base station has low receiving intensity and large fluctuation, which is different from the variation trend of the received power and distance of the reference signal outside the near-field area. From the antenna pattern of the base station antenna, it can be seen that the side lobe gain of the base station antenna fluctuates by 10 – 20 dB. The received power of the reference signal will be affected by both the gain of the transmit antenna and that of the receive antenna. It is indicated that the path loss model in this part of the region no longer follows the logarithmic fading model[14].

The path loss model divides the antenna coverage area into two parts based on the side lobe and main lobe coverage areas, which are referred to here as Area A and Area B. Segmentation is performed with Fresnel zone gaps in Ref. [15]. There are three ways to divide the propagation area:

1) The antenna coverage area is divided based on the side lobe and main lobe coverage areas, which is the distance of the line segment *OA* in Fig. 1. The distance of *OA* is given by:

$$d_1 = \frac{\Delta h}{\tan\left(\theta_1 + \frac{\theta_2}{2}\right)}. \tag{2}$$

2) The propagation area can be divided based on the center position of the main lobe of the antenna pattern, which is the distance of the line segment *OB* in Fig. 1. The distance to *OB* is given by:

$$d_1 = \frac{\Delta h}{\tan(\theta_1)}. \tag{3}$$

3) The propagation area can also be divided according to the Fresnel zone gap, and the distance is given by:

$$d_1 = \frac{4h_t h_r}{\lambda}. \tag{4}$$

3 Path Loss Statistical Modeling for Area A

The marshalling yard scenario tested is somewhat similar to the cutting scenario in rail transportation. The railway yard is located in the middle, with slopes and mountains covered with trees on one side and several workshops on the other side. According to the analysis, the received signal may be affected by direct waves, reflected waves, and scattered waves. The test area includes three base stations and nine cells. In the measurement, the transmitter uses a 5G AAU base station with an antenna gain of 24.5 dBi, the receiver uses a PCTEL horizontal omnidirectional antenna, and SPARK software is used for data storage and visual analysis. We select one of the cells for specific analysis.

An example of a single measurement result of the path loss after the antenna gain verification process of 150 cells in the marshalling station scenario is shown in Fig. 2. It can be seen from the figure that the path loss in the near-field area of the base station fluctuates greatly, which is different from the variation trend with a distance of the far-field area. When the conditions of 150 cells is substituted, it is calculated that *OA* = 154.64 m, *OB* = 214.66 m, and the Fresnel zone gap = 1212.17 m. From the actual test results in Fig. 2, it can be concluded that the boundary points in Definition (2) can better represent the boundary points of Area A and Area B, and the conclusions of other cells are similar. To sum up, Point B is divided as the breakpoint of the propagation area, and the models built in subsequent segmentation are based on this.

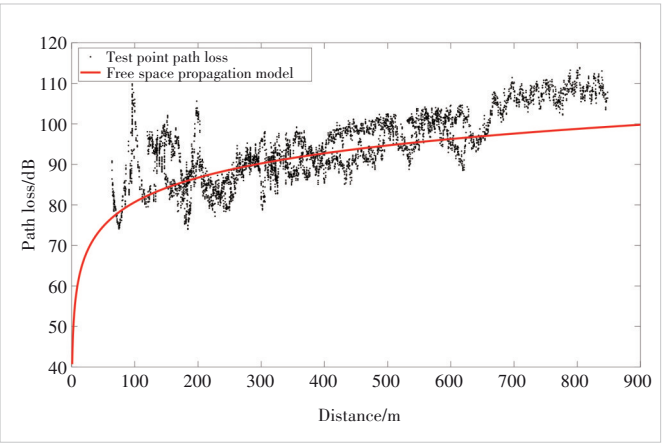

▲Figure 2. Path loss of 150 cells of the marshalling station

Due to the presence of a large number of metal products in the marshalling yard scenario, the influence of the reflection path in the near-field area is difficult to ignore. By contrasting the accuracy of the two-path model and the logarithmic fading model in Area A, we make statistics based on the path loss prediction error $e(i)$ of the sample points in each cell. The calculation formula of $e(i)$ is given by:

$$e(i) = PL_{\text{measure}}(i) - PL_{\text{predict}}(i), \tag{5}$$

where i denotes the cell sample point number, $PL_{\text{measure}}(i)$ is the i-th measured data sample, and $PL_{\text{predict}}(i)$ defines the i-th predicted data sample.

Under the same conditions, probability statistics are performed based on $e(i)$ of the path loss results predicted by the logarithmic fading model and the two-path model in the test cell of Area A. The corresponding cumulative distribution function (CDF) results are shown in Fig. 3. The average prediction error of the two-path model is 2.80 dB, and the standard deviation is 7.24 dB. The average prediction error of the logarithmic fading model is 4.75 dB, and the standard deviation is 8.26 dB. At the same time, it can be seen from Fig. 3 that in Area A, compared with the logarithmic fading model, the average prediction error of the two-path model is smaller and the change is more stable, which is more consistent with the actual measured data. Therefore, according to the calculation results, it can be concluded that in the marshalling station

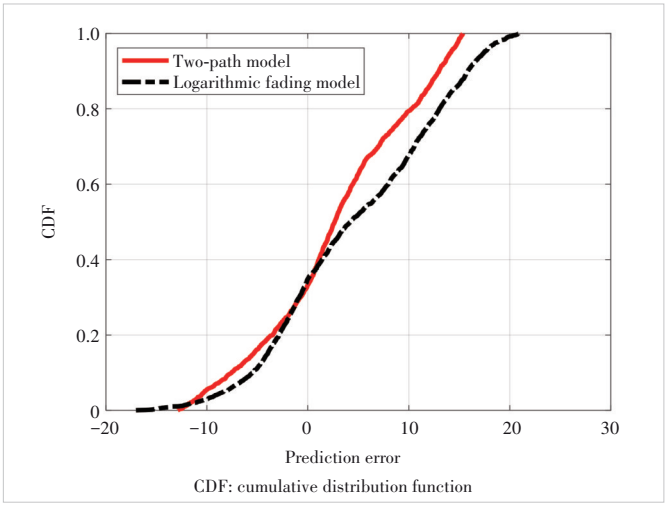

▲Figure 3. Prediction error statistics of marshalling yard Area A

scenario, the change of path loss in Area A obeys the two-path model. The received power of the two-path model is as:

$$P_r = P_t\left(\frac{\lambda}{4\pi}\right)^2\left|\frac{\sqrt{G_l}}{d_d} + \xi\frac{\sqrt{G_r}\,e^{-jk_\lambda(d_r-d_d)}}{d_r}\right|^2, \tag{6}$$

where d_d is the length of the direct path of the transmitter and receiver, d_r is the total length of the reflection path of the transmitter and receiver, k_λ is the wave number, and ζ is the reflection coefficient of the ground. In general, $\zeta=-1$, $G_l = G_a G_b$, and $\sqrt{G_l}$ is the total gain of the transmitting and receiving antennas on the direct path from the transmitter to the receiver; $G_r = G_c G_d$, and $\sqrt{G_r}$ is the total gain of the transmitting and receiving antennas on the reflective path from the transmitter to the receiver.

The fitting results of the two-path model are shown in Fig. 4.

4 Path Loss Statistical Modeling for Area B

In this section, an empirical model of large-scale fading of radio waves is established based on a large number of test samples obtained in the marshalling station Area B. Among them, the carrier frequency of the base station is fixed at 2.6 GHz, and the height of the receiver antenna is fixed at 1 m. We build a statistical model of Area B utilizing the path loss PL, the distance d of the transceiver antenna, and the height of the base station antenna h_t in the test data.

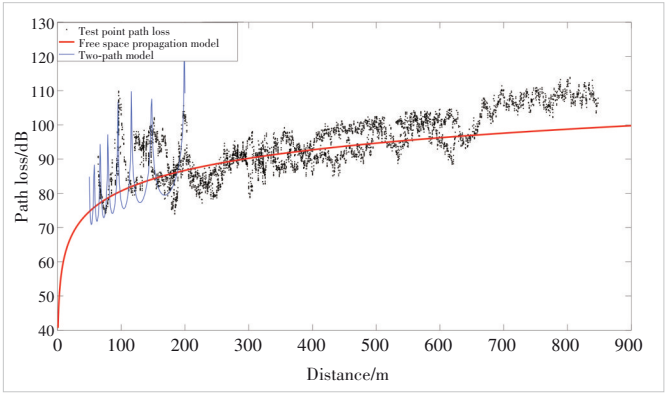

▲Figure 4. Fitting two-path model for path loss in marshalling station Area A

The path loss formula of the Hata model is as follows:

$$PL_{\text{Hata}} = 69.55 + 26.16\lg f_c - 13.82\lg h_t - \alpha(h_r) + (44.9 - 6.55\lg h_t)\lg d, \tag{7}$$

$$\alpha(h_r) = \begin{cases} (1.1\lg f_c - 0.7)h_r - (1.56\lg f_c - 0.8), & \text{medium and small cities} \\ 8.29\lg^2(1.54h_r) - 1.1, & \text{large city, } f_c \leqslant 200\ \text{MHz} \\ 3.2\lg^2(11.75h_r) - 4.97, & \text{large city, } f_c \geqslant 400\ \text{MHz} \\ 0, & h_r = 1.5\ \text{m} \end{cases}, \tag{8}$$

where f_c is the frequency (the unit is MHz), h_t and h_r define the effective heights of the transmitter antenna and the receiver antenna (the unit is m), and $\alpha(h_r)$ varies with the city size (medium and small cities; large cities) and frequency (≤ 300 MHz or >300 MHz).

In different scenarios, the Hata model changes the path loss model by adding a correction factor, and the expression after adding the correction factor is shown in Eq. (9).

$$PL_{\text{Hata}} = \Delta_1 + 74.52 + 26.16\lg f_c - 13.82\lg h_t - 3.2(\lg(11.75h_r))^2 + (\Delta_2 + 44.9 - 6.55\lg h_t)\lg d. \tag{9}$$

One part of the correction factors Δ_1 and Δ_2 in the Hata model is linear with the logarithm of the height of the transmitting antenna, and the rest are the constants in Table 1. The correction factors are given by:

$$\begin{cases} \Delta_1 = p_1\log_{10}(h_t) + q_1 \\ \Delta_2 = p_2\log_{10}(h_t) + q_2, \end{cases} \tag{10}$$

where p_1, p_2, q_1 and q_2 are the undetermined coefficients.

The correction factors Δ_1 and Δ_2 are fitted to the height of the base station antenna based on the calculation results. Taking the results of multiple tests as statistical data, we perform a least-square (LS) fitting model based on the path loss test data of nine cells. The fitting results are shown in Table 2.

▼Table 1. Correction factors of Hata model in different scenarios

Scenario	Correction Factor Δ_1	Correction Factor Δ_2
Urban area	−20.47	−1.82
Suburbs	$5.74\lg h_t - 30.42$	−6.72
Rural	$6.43\lg h_t - 30.44$	−6.71
Viaduct	−21.42	−9.62
Cutting	−18.78	$51.34\lg h_t - 78.99$
Station	$34.29\lg h_t - 70.75$	−8.86

According to the results of the nine cells in the marshalling yard scenario, we fit the optimal regression model under each cell through linear regression, including the corresponding constant term and path loss exponent n, and then calculate the corresponding correction factor for each cell. By conducting joint analysis of the height information of base stations in the corresponding cell, it is determined whether there is a significant linear relationship between the correction factors (Δ_1 and Δ_2) and the height of the base station antenna. The fitting results are shown in Figs. 5 and 6. The correction factors are given by:

$$\Delta_1 = -141.73, \tag{11}$$

$$\Delta_2 = 17.64\lg h_t - 17.22. \tag{12}$$

5 Validation and Evaluation

The empirical model proposed in this paper is compared with several traditional empirical models that are improved Hata models as well. The traditional empirical models including the Stanford University temporary model (SUI) and the Hata-Okumura extended model are selected as the reference model for comparison and verification. The validation data consist of three cells, and the validation data have the same measurement system as the statistical modeling data. The validation data are not used in statistical modeling, so they can be used to verify the accuracy and generalizability of the model.

▼Table 2. Fitting measurement results

Cell Number	Path Loss PL_0	Path-Loss Exponent n	Correction Factor Δ_1	Correction Factor Δ_2
62	4.565 0	4.513 81	−134.29	10.16
63	7.949 0	4.347 35	−131.07	9.25
64	3.651 2	4.358 74	−136.12	8.37
143	−3.014 8	4.542 59	−141.86	10.64
150	−7.115 8	4.472 55	−145.97	9.95
151	−4.066 2	4.482 93	−142.92	10.05
156	−4.460 3	4.442 59	−143.31	9.64
184	−13.105 2	4.438 65	−151.96	9.44
185	0.043 9	4.447 31	−138.89	9.53

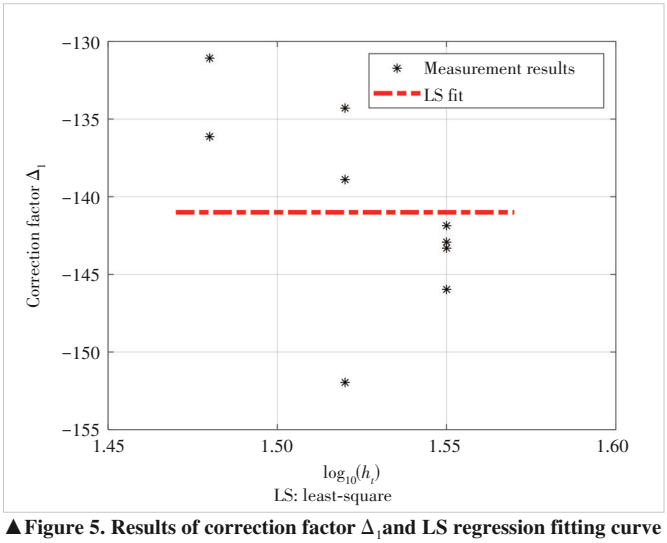

▲Figure 5. Results of correction factor Δ_1 and LS regression fitting curve

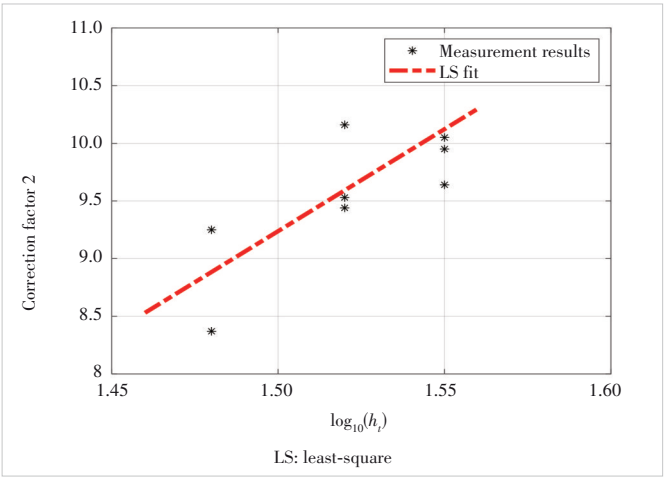

▲Figure 6. Results of correction factor Δ_2 and LS regression fitting curve

The SUI model, Hata-Okumura extended model and statistical model are represented by Model 1, Model 2 and Model 3, respectively. Fig. 7 shows a comparison of the accuracy of different models on the validation data at different prediction error sensitivities. When the maximum prediction error sensitivity is required to be 10 dB, the maximum prediction accuracy of the SUI model is 61.66%, that of the Hata-Okumura model is 59.55%, and that of the statistical model is 59.55% with an accuracy of 71.06%. In this scenario, compared with the existing SUI and Hata-Okumura models, the accuracy of the self-built statistical model is improved by about 11.06%. However, the prediction accuracies of the SUI model, the Hata-Okumura extended model and the self-built model in the marshalling yard scenario are not much different, indicating that the SUI model and the Hata-Okumura extended model have

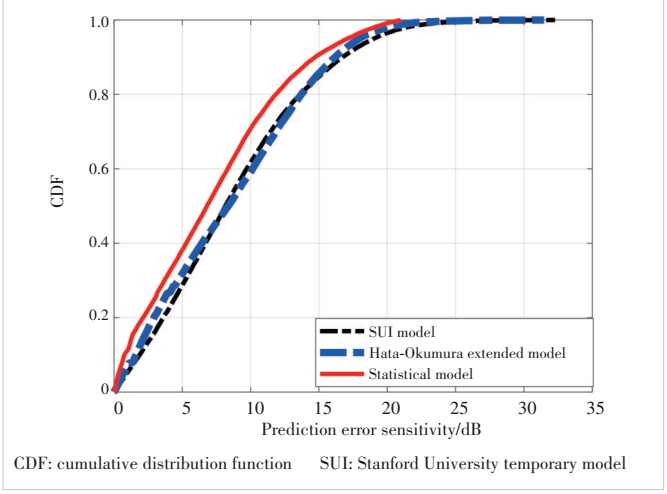

▲Figure 7. Accuracy comparison of different models based on validation data

certain applicable values in the marshalling yard scenario.

6 Challenges

In the statistical model, the path loss will increase with the growing of the distance between transceiver antennas as a whole. There is no need to consider detailed environmental information when the large-scale fading empirical model is applied to the scenario. In specific environments, such as railway marshalling yards, the transmission of radio waves may encounter fading and other conditions, resulting in changes in the final received power to reach the user, making it difficult to determine the specific value of the calculated path loss. This is also a deficiency of large-scale fading empirical models. In the future, it is hoped to re-validate predictions with the help of deterministic modeling, machine learning and other methods to achieve higher prediction accuracy.

7 Conclusions

In this paper, the calculation method of the propagation demarcation point for marshalling yard scenarios is proposed and verified to improve the accuracy of the subsequent empirical model. Based on numerous measured data, a large-scale path loss statistical empirical model for marshalling yard scenarios is established, and the propagation boundary point is regarded as the model segmentation point. The path loss in Area A conforms to the two-path model, and that in Area B is close to the logarithmic model. According to the measurement data in different cells, the correction factor in the marshalling yard scenario is fitted with the Hata model as the benchmark. Finally, the shortcomings and improvements that need to be made to the statistical model are discussed.

References

[1] AI B, MOLISCH A F, RUPP M, et al. 5G key technologies for smart railways [J]. Proceedings of the IEEE, 2020, 108(6): 856 – 893. DOI: 10.1109/JPROC.2020.2988595
[2] ZHONG Z D, GUAN K, CHEN W. Challenges and perspective of new generation of railway mobile communications [J]. ZTE Technology Journal, 2021, 27(4): 44–50. DOI:10.12142/ZTETJ.202104009
[3] AI B, GUAN K, RUPP M, et al. Future railway services-oriented mobile communications network [J]. IEEE communications magazine, 2015, 53(10): 78 – 85. DOI: 10.1109/MCOM.2015.7295467
[4] ZHAO Y J, ZHANG J Y, AI B. Applications of reconfigurable intelligent surface in smart High speed train communications [J]. ZTE Technology Journal, 2021, 27(4): 36-43. DOI: 10.12142/ZTETJ.202104008
[5] YANG M, HE R S, AI B, et al. Measurement-based channel characterization for 5G wireless communications on campus scenario [J]. ZTE communications, 2017, 15(1): 8 – 13. DOI: 10.3969/j.issn.1673-5188.2017.01.002
[6] LU J H, ZHU G, AI B. Radio propagation measurements and modeling in railway viaduct area [C]//6th International Conference on Wireless Communications Networking and Mobile Computing (WiCOM). IEEE, 2010: 1 – 5. DOI: 10.1109/WICOM.2010.5600926
[7] WEI H, ZHONG Z D, GUAN K, et al. Path loss models in viaduct and plain scenarios of the High-speed Railway [C]//5th International ICST Conference on Communications and Networking in China. IEEE, 2010: 1 – 5. DOI: 10.4108/iwoncmm.2010.3
[8] HE R S, ZHONG Z D, AI B. Path loss measurements and analysis for high-speed railway viaduct scene [C]//6th International Wireless Communications and Mobile Computing Conference. New York: ACM, 2010: 266 – 270. DOI: 10.1145/1815396.1815458
[9] NEWHALL W G, SALDANHA K J, RAPPAPORT T S. Propagation time delay spread measurements at 915 MHz in a large train yard [C]//IEEE Vehicular Technology Conference. IEEE, 2002: 864 – 868. DOI: 10.1109/VETEC.1996.501434
[10] KNORZER S, BALDAUF M A, FUGEN T, et al. Channel modelling for an OFDM train communications system including different antenna types [C]//64th Vehicular Technology Conference. IEEE, 2006: 1 – 5. DOI: 10.1109/VTCF.2006.55
[11] KNORZER S, BALDAUF M A, FUGEN T, et al. Channel analysis for an OFDM-MISO train communications system using different antennas [C]//66th Vehicular Technology Conference. IEEE, 2007: 809 – 813. DOI: 10.1109/VETECF.2007.178
[12] BRISO-RODRÍGUEZ C, FRATILESCU P, XU Y Y. Path loss modeling for train-to-train communications in subway tunnels at 900/2400 MHz [J]. IEEE antennas and wireless propagation letters, 2019, 18(6): 1164 – 1168. DOI: 10.1109/LAWP.2019.2911406
[13] TANG P. Channel characteristics for 5G systems in urban rail viaduct based on ray-tracing [C]//4th International Seminar on Research of Information Technology and Intelligent Systems (ISRITI). IEEE, 2022: 24 – 28. DOI: 10.1109/ISRITI54043.2021.9702771
[14] MOLISCH A F. Wireless communications [M]. Hoboken, USA: John Wiley & Sons, 2005
[15] WEN Y H, MA Y S, ZHANG X Y, et al. Channel fading statistics in high-speed mobile environment [C]//IEEE-APS Topical Conference on Antennas and Propagation in Wireless Communications (APWC). IEEE, 2012: 1209 – 1212. DOI: 10.1109/APWC.2012.6324963

Biographies

DING Jianwen received his MS and PhD degrees from Beijing Jiaotong University, China in 2005 and 2019, respectively. He is currently a professor of National Research Center of Railway Safety Assessment, Beijing Jiaotong University. He received the first prize of progress in science and technology of the Chinese Railway Society. His research interests are broadband mobile communications, dedicated mobile communication system for railway, and safety communication technology for train control system.

LIU YAO (21120095@bjtu.edu.cn) received her BE degree in communication engineering from Lanzhou Jiaotong University, 2021, China. She is currently working toward a master's degree with the State Key Laboratory of Rail Traffic Control and Safety, Beijing Jiaotong University, China. Her research interests include wireless communications and 5G-R.

LIAO Hongjian received his BE degree in communication engineering from Beijing Jiaotong University, China in 2020. He is currently working toward a master's degree with the State Key Laboratory of Rail Traffic Control and Safety, Beijing Jiaotong University, China. His research interests include wireless communications and 5G-R.

SUN Bin received his BS degree in electronic engineering and MS degree in electronic engineering from Beijing Jiaotong University, China in 2004 and 2007, respectively. From 2007 to 2015, he was a R&D manager with BeiJing LiuJie Technology Co., Ltd. He is currently an assistant researcher with National Research Center of Railway Safety Assessment, Beijing Jiaotong University. His main research interest is the interconnection and interworking of core network for dedicated railway mobile communication system.

WANG Wei is the LTE-R technical director and a railway wireless communication system expert of ZTE Corporation, with rich experience of the GSM-R system design. He has a deep understanding of GSM-R and LTE-R and has undertaken several major railway-related projects on wireless communication systems.